The United Nations University

GEOTHERMAL TRAINING PROGRAMME
Orkustofnun, Grensásvegur 9,
IS-108 Reykjavík, Iceland

Reports 1996
Number 2
IAEA Project ELS/8/005

TRACER MODELLING AND HEAT MINING CALCULATIONS FOR THE AHUACHAPÁN GEOTHERMAL FIELD EL SALVADOR C.A.

Francisco E. Montalvo L.
Comisión Ejecutiva Hidroeléctrica del Río Lempa (C.E.L.),
Centro de Investigaciones Geotérmicas (C.I.G.),
km 11 ½ Carretera al Puerto La Libertad,
Santa Tecla, La Libertad,
EL SALVADOR C.A.

ABSTRACT

Nine tracer test experiments using I^{131} and one using I^{125} were carried out in the Ahuachapán geothermal field during 1987 to 1992. In only six of the tests some tracer recovery was reported ranging from 0.1% to 28% for individual wells. In order to obtain a one-dimensional fracture flow model estimate of reservoir geometry parameters, several simulations were carried out using the TRINV code for selected tests that show the higher tracer recovery values. The simulations provide a support for the conceptual reservoir model as the tracer velocities in the southern upflow zone of the field, are more than 10 times higher than when the tracer is injected in the north-east part, where colder downflow influences the reservoir. The results of the tracer simulations were used as input for simulating heat mining from the reservoir during long term injection. A reservoir parameters sensitivity study was carried out using different values of porosity, injection temperatures, formation temperatures, constant and variable injection flow rates, fracture thickness and height. Additional high pressure steam and additional thermal power recovery due to the injection were also estimated. In some cases the results show an unexpectedly high cooling of the reservoir even at short distances between injection and production wells (≈350 m). An electrical power recovery of 0.1 MW is estimated at lower injection flow rates (1-2 kg/s) of 160°C water.

1. INTRODUCTION

The Ahuachapán-Chipilapa geothermal system is associated with the southern flank of the Central Salvadorean Graben, and located at the northwest sector of the Laguna Verde volcanic group. A complex volcanic extrusive structure was developed during Quaternary times near the Pliocene tectonic block of Tacuba-Apaneca volcanic chain. The regional fault system controlled first the sinking of the graben and subsequently the eruption of volcanic products. Today 32 wells have been drilled in the Ahuachapán area and a power plant, now with 95 MWe installed capacity, has been in operation since 1975.

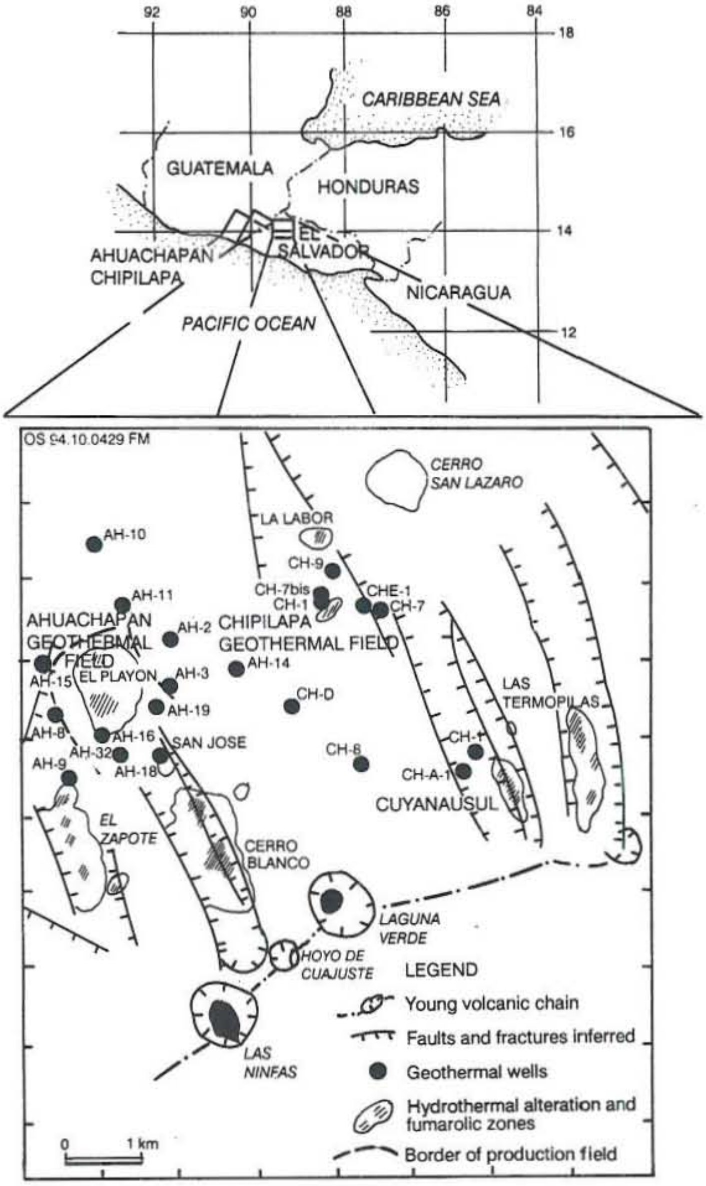

FIGURE 1: An overview of the Ahuachapán-Chipilapa geothermal system

The Ahuachapán and Chipilapa geothermal fields seem to be driven by the regional tectonic evolution with a fresh fracturation zone. Hydrothermal alteration and fumarolic zones, are distributed across an area of 50 km^2 (Figure 1). The regional and local structures are controlled by a system of faults and fractures oriented along three directions:

- E-W which is approximately the trend of the main graben;
- The west sector of the field is bound by a second system of faults oriented NE-SW;
- Surface geothermal activity is associated with the most recent faults and fractures with NNW-SSE trend.

The stratigraphic sequence of the Ahuachapán area consists mainly of tuff and lavas (upper part) of 200 m thickness, young agglomerates (cap rock) up to 400 m thick, Ahuachapán andesites (geothermal reservoir) with thickness up to 300 m and older agglomerates (basement).

Reinjection is considered to be an integral part of the future production strategy for the numerous geothermal reservoirs that are presently under exploitation. The main benefit of the reinjection is the reservoir pressure recovery generally obtained. This benefit may, however, disappear if rapid thermal breakthrough follows the reinjection. Substantial reinjection and numerous injection experiments have taken place in Ahuachapán. It is of interest to analyse this data and especially try to estimate the benefit of the injection. The scope of the present work is to analyse the tracer experiments already carried out in order to gain knowledge on the different fluid flow paths in the Ahuachapán reservoir. This provides an estimate of some critical reservoir parameters and finally allows one to evaluate the influence of injection on the productivity of the reservoir.

2. THE AHUACHAPÁN GEOTHERMAL FIELD

The Ahuachapán field is a liquid-dominated reservoir with temperatures in the range 210-240°C. It is located in a tectonically active zone where the movement of fluids is conducted mainly by a fault structure system. The well field covers an area of 4 km^2 with 32 drilled wells varying in depth from 591 to 1524 m. Their average elevation is around 800 m a.s.l. At present there are 14 production wells. The remaining wells are mainly used for monitoring and for injection (Montalvo, 1994; Quijano, 1994).

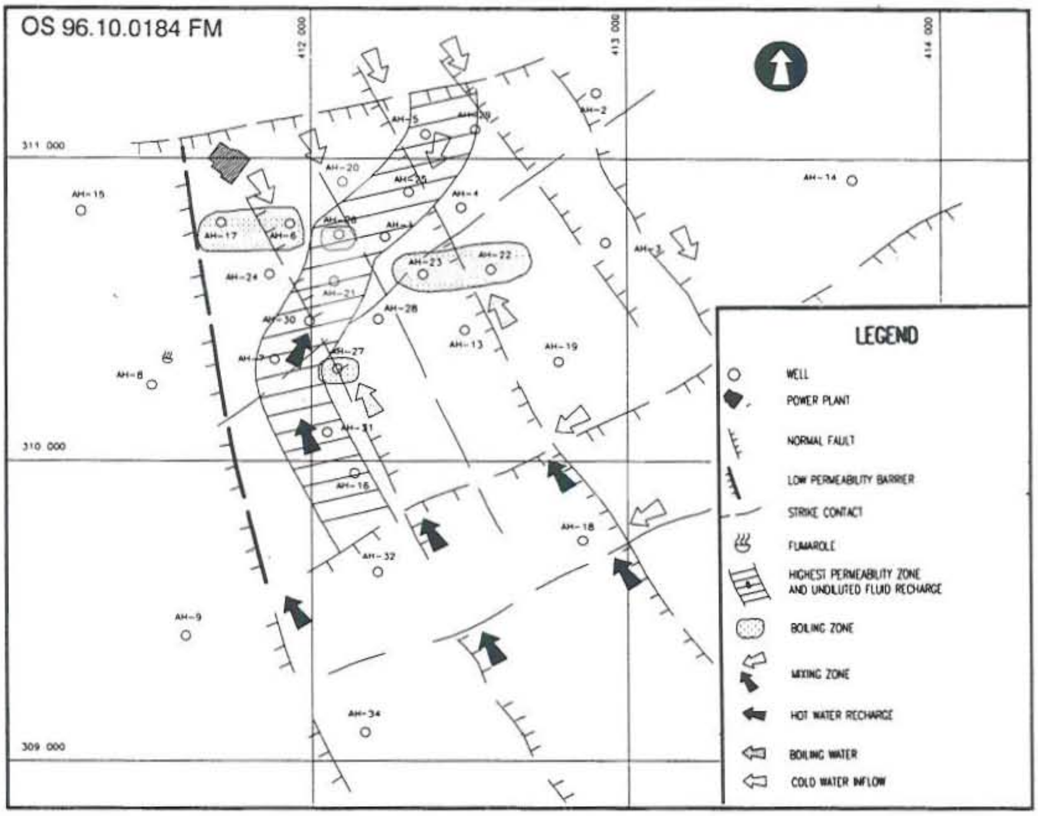

FIGURE 2: A conceptual model of fluid flow for the Ahuachapán geothermal field (Montalvo, 1996a), black arrows represent the hot fluid recharge, the white ones the "cold" water inflow and the gray areas zones of boiling

A large scale injection project was carried out from 1975, when commercial exploitation of the field started, until 1982. Since then only minor injection has taken place mainly during tracer tests. The separated water has been eliminated using two alternatives: 1) By injection into the reservoir at separation pressure (6 bar). The injection was stopped in 1982 due to a temperature decline in some wells. 2) Surface waste along a 80 km long concrete channel to the Pacific Ocean. A water injection temperature of 160°C has been used since 1982 during channel maintenance but only for few days annually and for the tracer experiments.

Taking into account the high mass extraction rate and pressure decline in the Ahuachapán well field, several studies including reservoir modelling and tracer test experiments have been carried out in order to optimize the exploitation strategy (ELC, 1993; Bustillo, 1996; CEL internal reports). The reservoir modelling studies revealed the convenience of developing further the southern part of the field for production purposes and use the nearby Chipilapa field as an injection zone.

3. TRACER TEST DESCRIPTION AND CONCEPTUAL FLOW MODELS

In order to study the hydrological recharge paths to the Ahuachapán reservoir, to locate feedzones and to evaluate different injection sites, several tracer test experiments have been carried out from December 1987 until December 1992. Nine tracer tests using the radioactive isotope I^{131} (half life of 8 days) and one experiment using I^{125} (half life of 60 days) were carried out. In eight of the experiments the tracer was injected into wells AH-2, AH-5 and AH-29 located in the NNE sector of the well field (Figure 2). This area has been identified in the conceptual reservoir model as an outflow zone of the geothermal fluid and in the production models as a recharge zone of "cold" water (Montalvo, 1994). Only two tracer injection experiments have been carried out in the S-SE part of the well field into wells AH-32 and AH-18. This part of the area is mainly related to hot fluid recharge to the system (Steingrímsson et al., 1991). In half of the tracer experiments a constant injection flow rate was used in the range 38-49 kg/s but for short periods of time, less than 3 months for the I^{131} experiments and about 6 months for the test using I^{125}.

A conceptual reservoir model of the Ahuachapán field is shown on Figure 2. It is based on geological structural information, fluid chemistry and reservoir properties. The model shows the main fault system, a high permeability zone, boiling and mixing zones and the movement of different chemical fluids entering the well field (Montalvo, 1996a).

4. TRACER TESTS AT AHUACHAPÁN WELL FIELD, SAMPLING, ANALYSIS AND RESULT

The general procedure for the Ahuachapán tracer tests has been as follow. Few days before the tracer injection, two litre fluid samples are taken for background radiation analysis from production wells and surface springs that are expected to be in hydrological communications with the reservoir. Usually the fluid sampling from the observation wells commence on the day of tracer injection with up to eight daily samples in the first month, one sample on every day for the next two weeks and finally the sampling frequency is reduced to three times a week for the last two weeks for the short term experiments using I^{131}. The sampling frequency for the long term experiment using I^{125} was less systematic or generally around two-three samples per well in each week during the six months monitoring period. Some down-hole fluid samples were collected in few cases, but the results were not significant and not interpretable. The same applies for the spring results which gave no positive tracer response. Only few of the tracer tests showed a good tracer returns in observation wells. General information on some selected tracer tests is given in Table 1.

TABLE 1: A summary of the selected tracer tests considered in this study

Test #	Well	Latitude (m)	Longitude (m)	Elevat. m a.s.l.	Depth (m)	Main feed zones 2Phase (m)	Main feed zones Liquid (m)	Prod. (kg/s)	Inject. (kg/s)
1	**AH-5(i)**	311084,1	412362,9	789	952	515-590	720-920		9,6
	AH-1(r)	310743,5	412233,7	803	1195	500-550	?	55	
	AH-20(r)	310924,4	412092,9	793	850	460-500		43,9	
4	**AH-29(i)**	311100,1	412515,5	795	1200	570-680	840-870,1140		49
	AH-1(r)	310743,5	412233,7	803	1195	500-550	?	49,8	
	AH-5(r)	311084,1	412362,9	789	952	515-590	720-920		
	AH-20(r)	310924,4	412092,9	793	850	460-500		58,2	
	AH-22(r)	310635,5	412564,6	843	660	500-520	600		
10	**AH-2(i)**	311222,7	412603,5	808	1200		700-1200		38
	AH-1(r)	310743,5	412233,7	803	1195	500-550	?	58,9	
	AH-19(r)	310331	412765,2	873	1416	700-770	1100-1370	46,9	
	AH-20(r)	310924,4	412092,9	793	850	460-500		59,5	
	AH-22(r)	310635,5	412564,6	843	660	500-520	600	16,4	
	AH-23(r)	310622,3	412351,9	825	924	460-525		31,3	

i are injection wells; r are observation wells with tracer return

TABLE 2: Summary for selected tracer tests in Ahuachapán

Test number:	**1**	**4**	**10**
Tracer injected:	I-131	I-131	I-125
Tracer concentration:	0.81 Ci = 29.97 GBq	2 Ci = 74 GBq	0.47 Ci = 17.4 GBq
Injection date:	11 December 1987	30 June 1989	16 December 1992
Injector well:	AH-5	AH29	AH2
Injection flow rate:	35 m3/h (pulse)=9.7 kg/s	176.4 m3/h=49 kg/s con. rate	38 kg/s (constant rate)
Monitoring wells:	AH1, AH5, AH6, AH20, AH21, AH27, AH28, AH31	AH1, AH2, AH5, AH6, AH17, AH19, AH20, AH21, AH22, AH23, AH24, AH26, AH27, AH28, AH31	AH1, AH6, AH7, AH17, AH19, AH21, AH22, AH23, AH26, AH 27, AH 28, AH31
Recovery total %:	30%	8,57%	6.64%
Monitoring time:	76 days	76 days	197 days

After the sampling, the next step is to recover in the laboratory the pure iodide from the 2 litre water sample using chemical technics (separation, gravimetric quantification and specific ion electrode determination). Subsequently a liquid scintillation counter (Packard TriCarb 1500 LSC) gives the recovery of radioactive iodide from the water samples. The calculations are based on the "counts per minute" values minus background values and corrected for radioactive decay, volume of the sample taken, yield of iodide and the efficiency of the counting. The tracer concentration is expressed as a fraction of tracer recovered per day (amount of tracer per litre of water being discharged divided by the total amount of tracer injected). As this number is very small it is often multiplied by 10^{12} (McCabe, 1987; 1991). The cumulative tracer recovery is finally obtained by multiplying the concentration results of the samples (L^{-1}) by the water flow rate of each monitoring well.

TABLE 3: Tracer breakthrough time, velocities and recoveries for the selected tests

Test #	Well dipole	Distance (m)	Tracer break-through (days)	Max. tracer velocity (m/d)	Recovery (%)	Maximum concentrat. ($L^{-1}*10^{12}$)
1	AH5-AH1	350	4	88	28,00	1930
3	AH29-AH1	450	5	90	0,130	15,9
	AH29-AH20	455	12	38	0,011	1,64
	AH29-AH22	469	8	59	0,002	1,23
4	AH29-AH1	450	4	113	3,560	242
	AH29-AH5	156	1	156	0,420	515
	AH29-AH20	445	1	445	4,580	69
	AH29-AH22	460	4	115	0,015	23
6	AH2-AH1	820	10	82	0,406	35
	AH2-AH5	540	9	60	0,622	90
	AH2-AH19	910	15	61	0,485	40
	AH2-AH20	830	16	52	0,021	5
	AH2-AH22	670	15	45	0,216	80
	AH2-AH23	810	18	45	0,031	35
8	AH32-AH1	1030	7	147	0,105	31
	AH32-AH6	1095	4	274	0,010	55
	AH32-AH19	845	3	282	0,002	27
	AH32-AH20	1275	3	425	0,117	4
	AH32-AH22	990	5	198	0,002	24
	AH32-AH23	920	3	307	0,057	36
	AH32-AH24	970	4	242	0,002	44
	AH32-AH26	1040	5	208	0,043	20
	AH32-AH27	615	4	154	0,017	20
	AH32-AH31	425	24	18	0,028	2
	AH32		4		58,710	424360
10	AH2-AH1	820	10	82	2,540	37
	AH2-AH20	860	16	54	0,810	28
	AH2-AH22	670	12	56	1,020	96
	AH2-AH23	810	19	43	0,460	27

Tables 2 and 3 present a summary of the selected tracer tests and field data results. The recovery curves will be analysed here by using parameters like production and injection flow rates, distances between

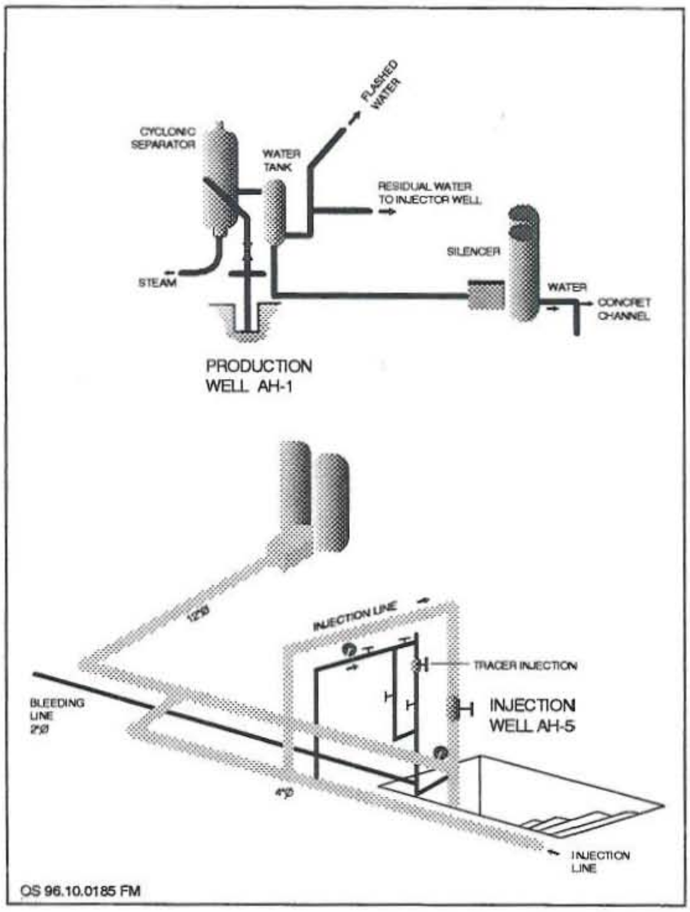

FIGURE 3: Surface installations for the injection well, monitoring well and tracer injection line

wells, maximum tracer concentration and time, and half-width of the recovery curve. All the relevant information for the ten experiments that have been carried out at the Ahuachapán geothermal field using radioactive iodide are summarized in the supplementary Appendix of this report (Montalvo, 1996b). Figure 3 shows the typical design of the surface equipment that was used for the tracer injection.

Field-laboratory data results show very rapid tracer breakthrough times for some wells ranging from one day up to a week (Table 3). The lowest observed tracer velocity in the field is 38 m/d and the highest is 445 m/d (Figures 4 and 5). They are registered in opposite tracer injection locations: the low velocities at the northern sector of the Ahuachapán well field, and the high velocities when injecting in the southern part. The tracer recovery is generally very low, ranging from less than 1% to a maximum of 28% in well AH-1 for the tracer injected into well AH-5 (Figure 6).

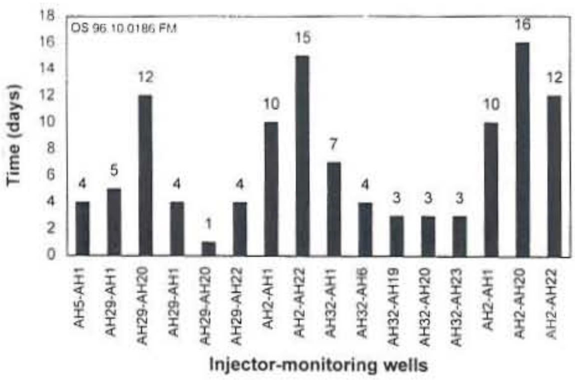

FIGURE 4: Tracer breakthrough times for selected tests in Ahuachapán

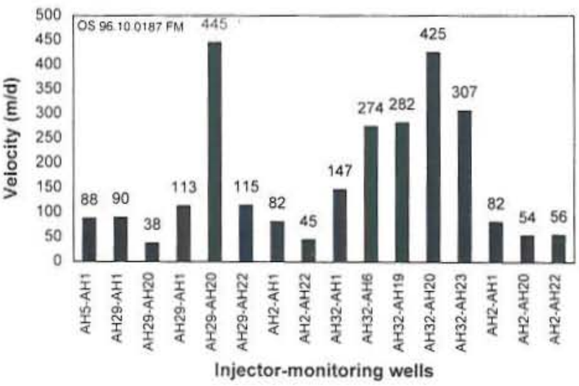

FIGURE 5: Maximum tracer velocities in Ahuachapán

5. TRACER MODELLING

There are different models for the simulation of tracer results. The input in using these simulators is almost the same, some reservoir parameters and how much of the tracer material was recovered etc. The cumulative tracer recovery is represented by the following equation:

$$\int_0^\infty [C(t) - background]\, dt \qquad (1)$$

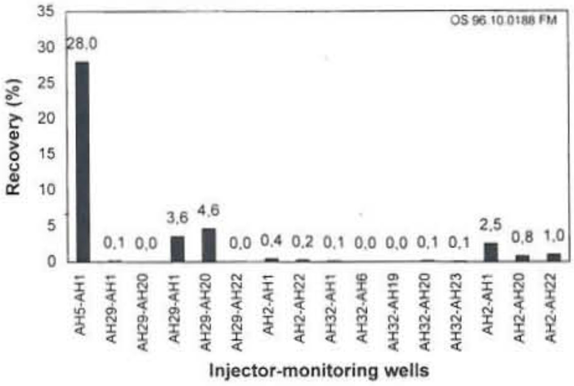

FIGURE 6: Cumulative tracer recovery in Ahuachapán

Some types of models that can be applied for the tracer results are:

- Infinite horizontal layer, bounded by impermeable formation;
- Simple fracture model;
- Distributed parameters model (AQUA).

This report shows the application of the simple fracture model as an approach of the production-injection well dipole scheme.

6. TRINV PROGRAM

The TRINV code (Arason and Björnsson, 1994) has been applied in order to simulate tracer data and provide an estimation of some reservoir parameters like cross-sectional area of the 1-D flow channel (fracture) conducting the tracer between wells ($A\phi$ = m^2), its longitudinal dispersivity (αL = m), dispersion coefficient (D = m^2/s), mean velocity of flow (μ = m/d), mass recovery (%) etc.

The input used is the total production of the monitoring well (Q = kg/s), injection flow rate in injector well (q = kg/s), distance between wells (x = m), total injected mass of tracer (C = kg), maximum concentration of tracer, the time of maximum concentration (t_m = days), half width of the recovery curve (w = days), number of possible flow paths connecting the wells, density of reservoir water (970 kg/m^3) and density of water in laboratory (998 kg/m^3). Tracer concentration units are in kg/m^3.

First of all, an initial guess of the model parameters is applied with observed concentration data providing a model of variable complexity. The code uses a non-linear least squares solutions algorithm for the model parameters. Inverting for the tracer recovery curve in a production-injection well dipole produces a "best" fracture flow model. Finally, graphs of observed and calculated data for the individual tracer pulses are made.

The basic assumptions for the simple fracture model are:

- Flow channel between wells is along a narrow fracture zone;
- One-dimensional flow model;
- Neglected molecular diffusion;
- Assuming constant injection-production flow rates.

6.1 Governing equations

The governing differential equation describing tracer concentration in a one-dimensional flow channel is written as

$$D\frac{\partial^2 C}{\partial x^2} = \mu\frac{\partial C}{\partial x} + \frac{\partial C}{\partial t}; \qquad \mu = \frac{q}{\rho A \phi} \tag{2}$$

where D is the dispersion coefficient of the flow channel $(= \alpha_L \mu)$. The cross-sectional area for the flow channel is A = h×b (height and thickness of the channel).

The tracer concentration is correlated to the fracture zone concentration by using conservation of tracer mass flow

$$c \times Q = q \times C \tag{3}$$

where c is the tracer concentration of the produced fluid, C is the tracer concentration in the fracture, Q is the production flow rate and q the injection flow rate.

The solution for the governing equation is

$$c(t) = \mu\frac{M}{Q}\frac{1}{2\sqrt{\pi D t}}\exp\frac{-(x-\mu t)^2}{4Dt} \tag{4}$$

A correction is also needed for converting tracer concentrations at the weirboxes (C_w) to tracer concentrations at reservoir conditions (C_r). Using the water flow rate in weirbox (W) and the injection flow rate (q), the correction equation is:

$$C_r = \frac{C_w \times w}{q} \tag{5}$$

6.2 Tracer return profiles and simulations

The following chapter presents a discussion on the conceptual reservoir model using the TRINV velocity results and the comparison with the field data. The recovery curve and simulated curves for the Test #1 are presented in Figure 7. As mentioned before, the 20% recovery for well AH-1 represents the highest recovery for all the experiments at Ahuachapán.

The simulation in Figure 7b, gives a determination coefficient of 97%, using three main flow channels connecting the two wells. This could reflect two fractures channelling most of the flow and a matrix flow channel for the third and the widest pulse. Its presence became necessary in the simulation in order to fit the tail of the tracer recovery curve. The mean flow velocity in the first channel is around 19 m/d (Figure 7b), compared with velocity tracer breakthrough time which is 88 m/d. The average velocity for all the three channels is 12 m/d. The reason for the difference is that the TRINV velocity corresponds to the mean tracer velocity, whereas the field data takes the first arrival in the recovery curve. The cumulative tracer recovery is 28.2 % for the simulated data, the longitudinal dispersivity for all the channels is around 210 m and the cross-sectional area of the fracture is 79 m^2.

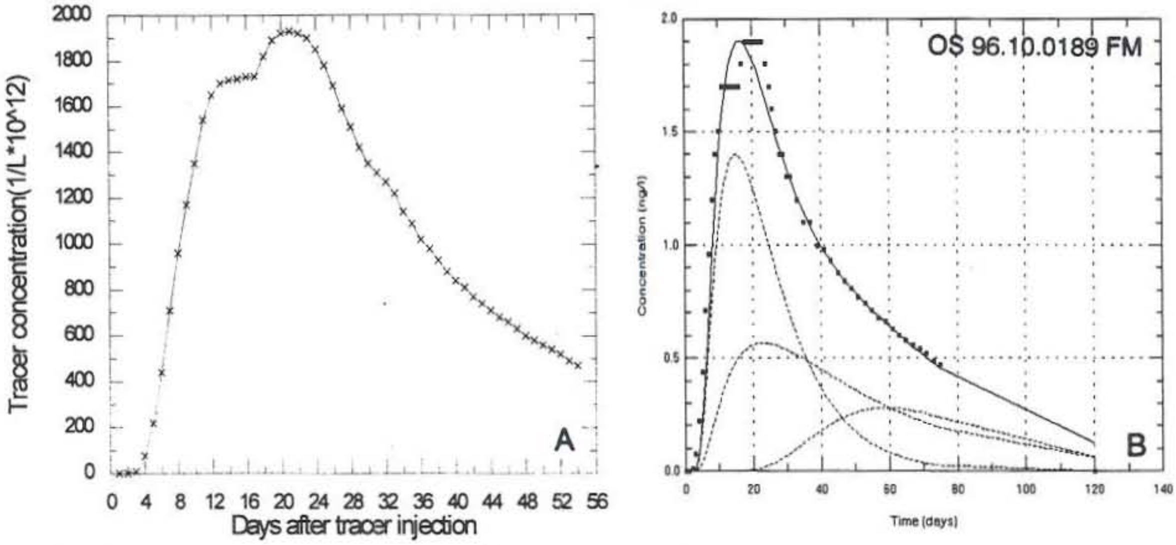

FIGURE 7: Test #1, a) Tracer recovery curve; b) Measured and calculated tracer recovery for the AH-1→AH-5 dipole

These results may indicate that the higher dispersivity values are due to the presence of several fractures (in this case two) between the wells as shown by Figure 8, related to the production-injection well dipole (Axelsson et al., 1995).

Figure 8 shows the lithology and main geological features of the different layers between AH-1 and AH-5, their elevation, the distance between the wells, the production and injection flow rates used for the experiment, circulation losses, feed zones and suggested tracer flow in the two channels.

Figures 9-13 present some selected recovery curves and corresponding simulations for Test #3 (AH-29 → AH-20), Test #4 (AH-29 → AH-1), Test #8 (AH-32 → AH-6), and the long term experiment Test #10 (AH-2 → AH-22). In almost all the simulations, the coefficient of determination is higher than 90%.

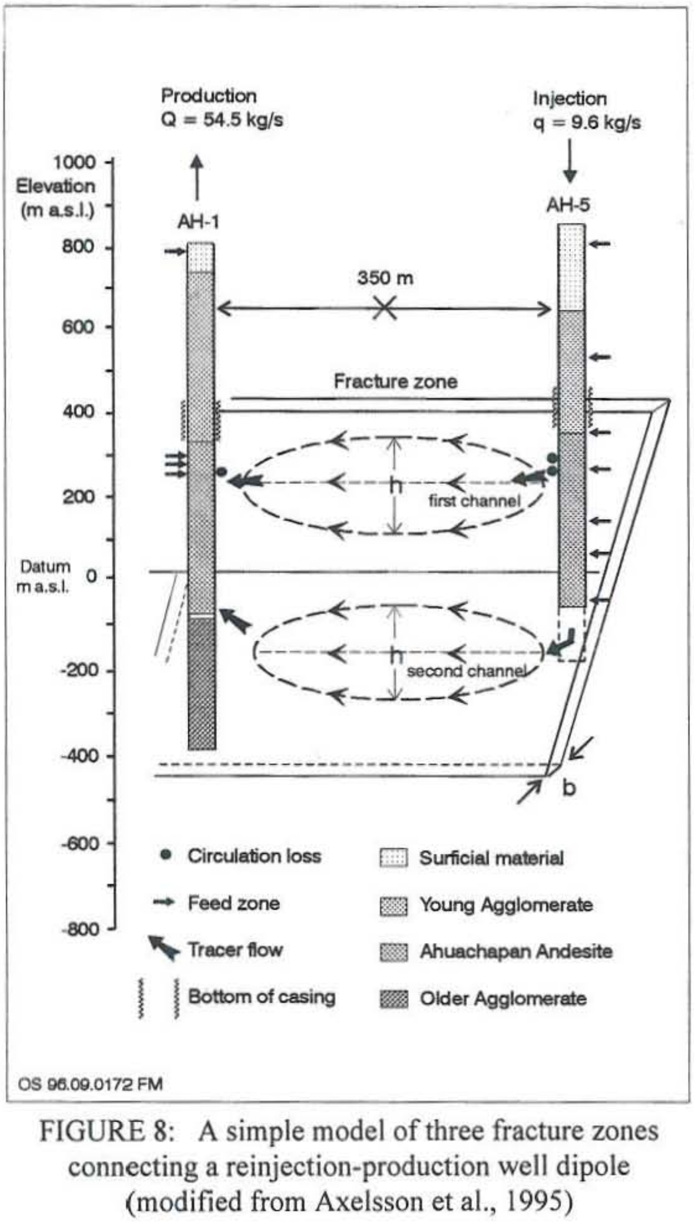

FIGURE 8: A simple model of three fracture zones connecting a reinjection-production well dipole (modified from Axelsson et al., 1995)

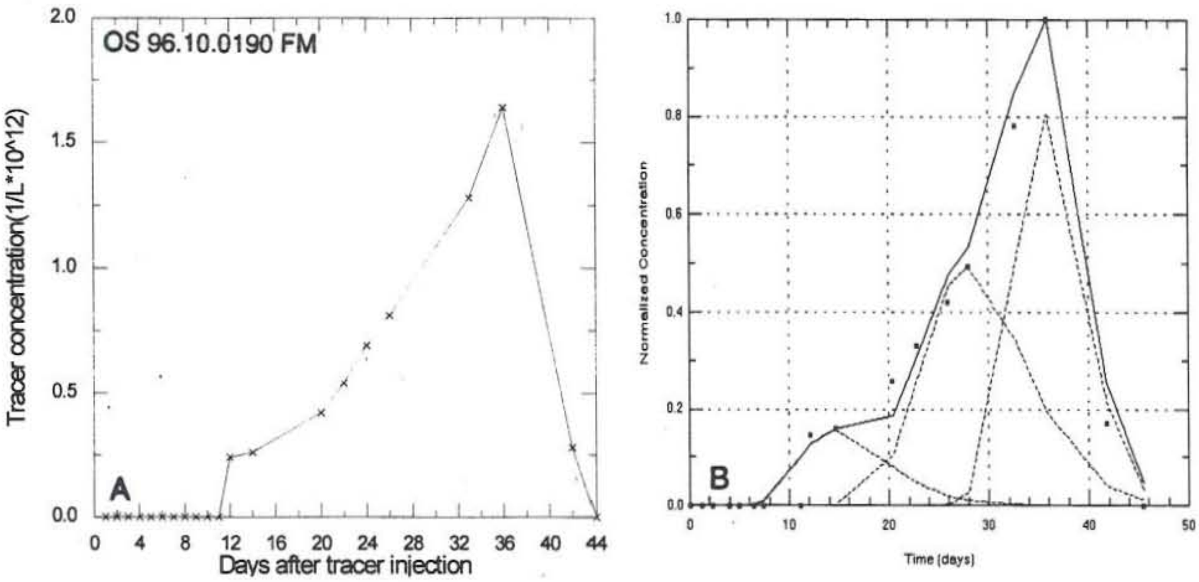

FIGURE 9: The well dipole AH-29→AH-20 (Test #3), a) Tracer recovery curve; b) Measured and calculated tracer recovery

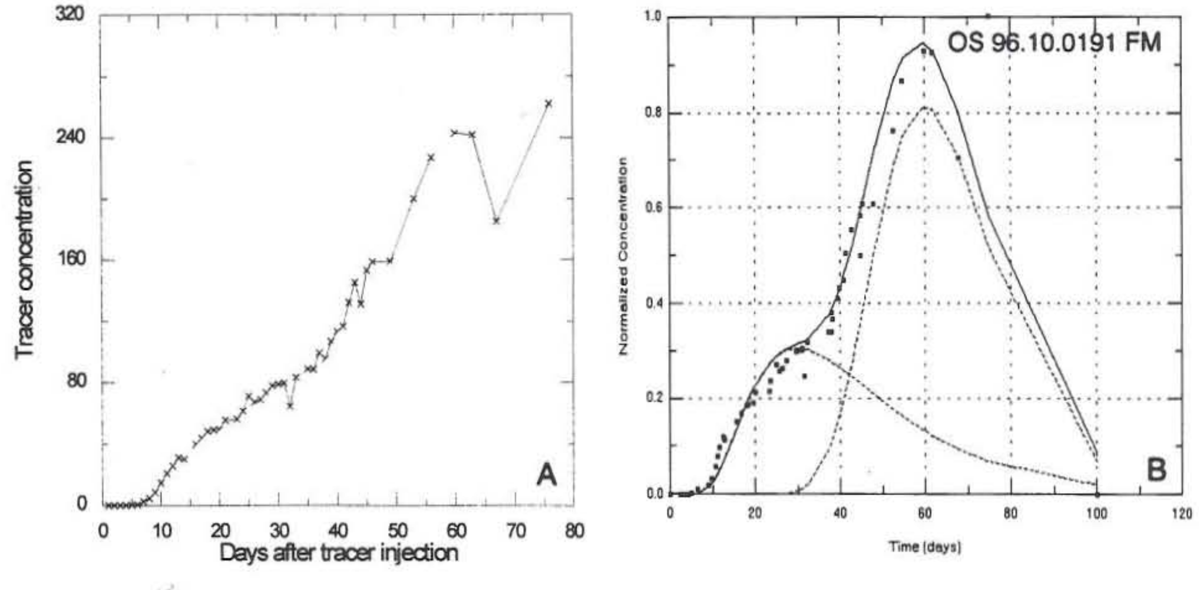

FIGURE 10: The well dipole AH-29→AH-1 (Test #4), a) Tracer recovery curve; b) Measured and calculated tracer recovery

The low tracer recovery and the scattered tracer recovery lead to low values for the fracture cross section area Aϕ and are assumed to reflect low confidence for the interpretation of the fracture model and also for the cooling and thermal efficiency predictions (see next chapter). Because the tail of the tracer recovery curves is often missing, in some cases it has been necessary to set a zero concentration in order to simulate the end of the recovery curve.

In the case of Test #8 (Figures 11 and 12) the tracer was injected into well AH-32. Only four days later the well was put into production and most of the tracer (58.7 %) flowed back from the well. However, some information related to this experiment is valuable, at least in the qualitative point of view and will be discussed in the next chapter.

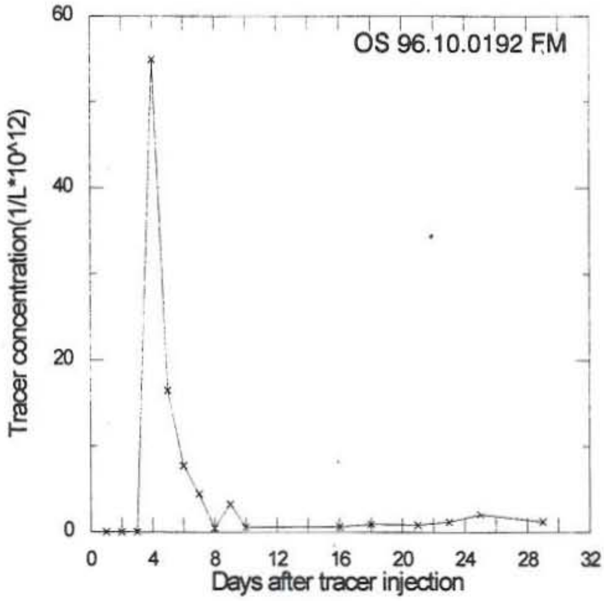

FIGURE 11: Tracer recovery curve for the well dipole AH-32→AH-6 (Test #8)

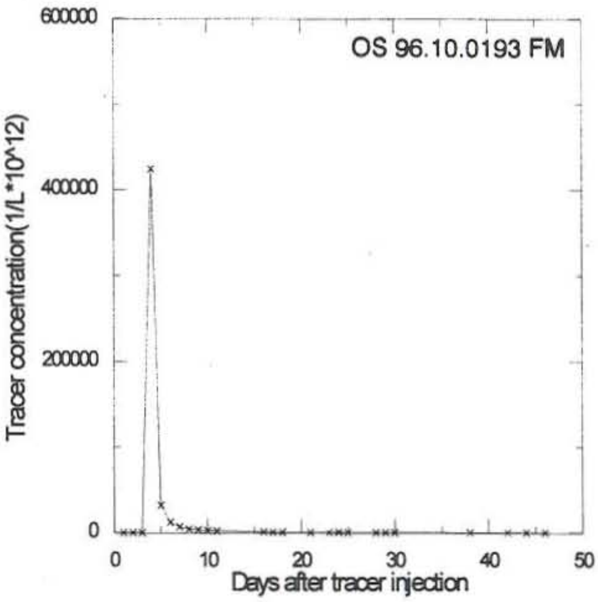

FIGURE 12: Tracer back flow from well AH-32 (Test #8)

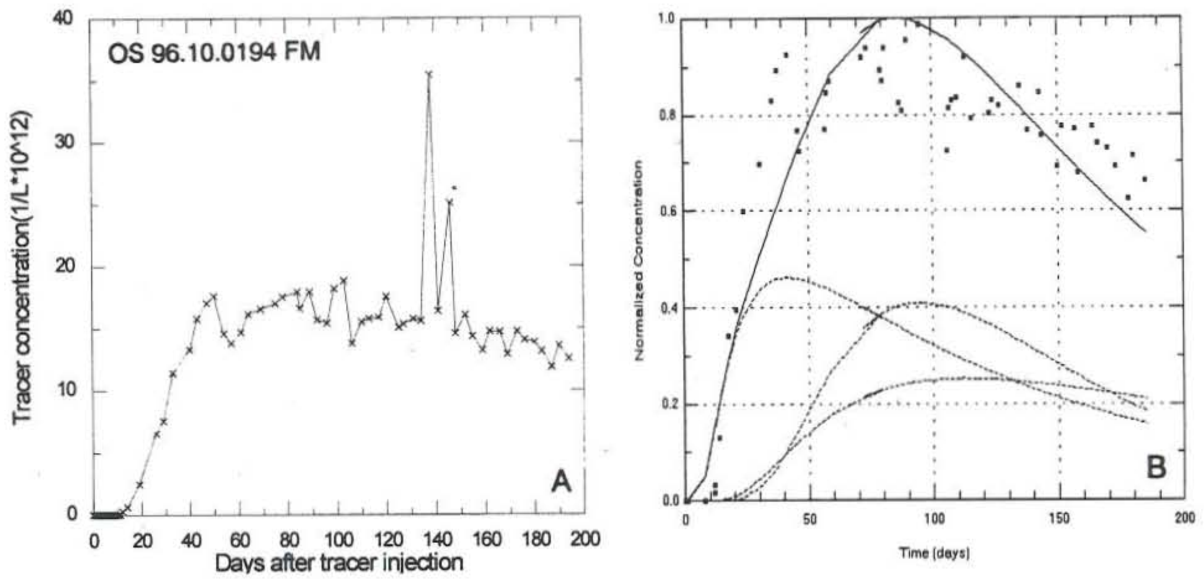

FIGURE 13: The well dipole AH-2→AH-22 (Test #10), a) Tracer recovery curve; b) Measured and calculated tracer recovery

The long term experiment using I^{125} (Figure 13) shows almost the same results as the short term experiment using I^{131}, reporting also low tracer recovery values and scattered data that made the simulations difficult, resulting in very low values for the cross-sectional area of the proposed fracture connecting the wells. We must also take into account that the low cumulative recovery tests and their scattered results could indicate high mixing volume for the tracer (matrix flow) also reflected by the higher dispersivity values.

More details about the different results for several simulations are in the Appendix to this report (Montalvo, 1996b). Figures 14, 15 and 16 show graphically some of these results.

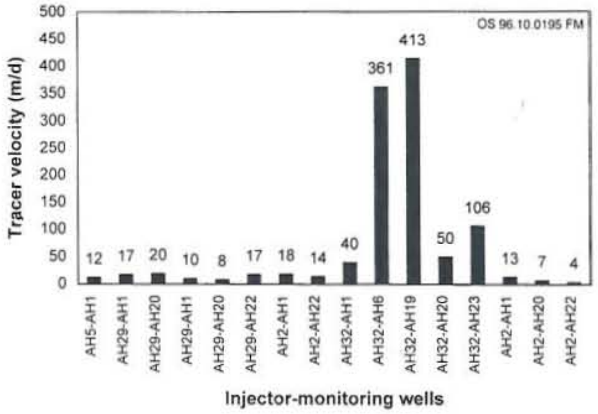

FIGURE 14: Tracer velocities from TRINV simulations for selected well dipoles

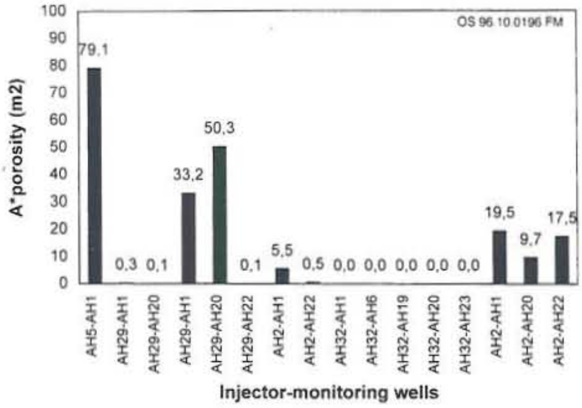

FIGURE 15: Sum of cross-sectional areas by TRINV simulations for selected well dipoles

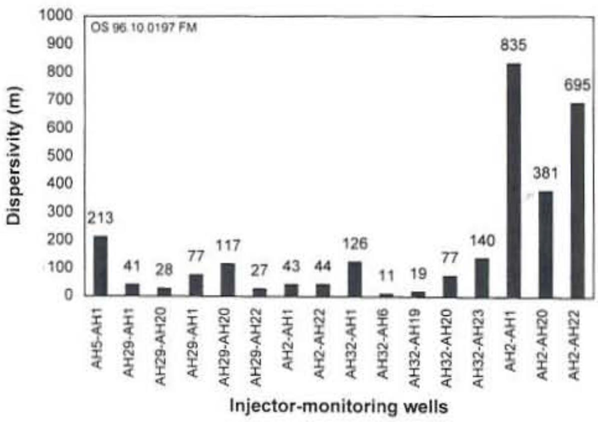

FIGURE 16: Tracer dispersivities from TRINV simulations for selected well dipoles

TABLE 4: Main results produced by TRINV simulations for selected wells dipole

Test #	Well dipoles	v (m/d)	mr (%)	a*l (m)	A*p (m^2)
1	AH5-AH1	11,9	28,20	213,1	79,08
3	AH29-AH1	17,1	0,13	41,3	0,28
	AH29-AH20	19,5	0,01	28,2	0,07
4	AH29-AH1	10,1	3,56	77,1	33,16
	AH29-AH20	8,0	4,58	116,7	50,28
	AH29-AH22	17,3	0,02	27,3	0,08
6	AH2-AH1	18,5	0,42	43,1	5,53
	AH2-AH22	13,6	0,24	43,6	0,54
8	AH32-AH1	39,7	0,10	126,2	0,02
	AH32-AH6	361,4	0,01	10,9	0,00
	AH32-AH19	413,2	0,00	18,8	0,00
	AH32-AH20	50,0	0,12	76,5	0,02
	AH32-AH23	106,0	0,06	139,5	0,01
10	AH2-AH1	13,1	2,53	834,7	19,50
	AH2-AH20	7,1	1,14	381,1	9,71
	AH2-AH22	4,2	1,03	694,5	17,46

Table 4 summarizes the results of the simulations for the mean velocities (μ = m/d), mass of tracer recovered (mr %), the tracer dispersivity (α_L = m) and the sum of the cross-sectional area for the fractures connecting injection and production wells ($A\phi = m^2$).

7. PREDICTING THE THERMAL EFFICIENCY OF INJECTION

The analysis of the tracer recovery data presented in the last chapter provides a valuable insight into the geometrical properties of the flow channels that connect injection and production wells in Ahuachapán. This is the flow channel cross-sectional area $A\phi$. Given that the flow channel is a fracture of a width b and height h, one can predict analytically the temperature of the injected water flowing in the fracture. In the following sections the computer program TRCOOL is presented (Arason and Björnsson, 1994) and the governing equation of the heat flow calculation. Finally, the tracer flow cross-sectional areas, $A\phi$, are applied for studying the thermal efficiency of the injection in Ahuachapán.

7.1 Basic assumptions and equations

The TRCOOL program was used to estimate the cooling of the Ahuachapán reservoir and to predict the additional steam gained by the injection of colder fluid and hence the additional electrical power recovered. Several sensitivity analysis were made using different values for the temperature of the injected water (Tinj), formation temperature (Tfor), injection flow rate (q), porosity of the fracture (ϕ), width of the fracture zone (b) and height of the fracture zone (h).

The following assumptions are made on the heat flow calculations to a fracture zone in the TRCOOL calculations:

- Analysis of tracer return profiles provide an estimate of the cross-sectional area A of the flow channel and the total contact area between the reservoir rock and the flow channel;
- The temperature of the injected fluid at any distance along the flow channel can be estimated by considering the heat convected along and conducted to the flow channel.

The main equations solved by the program are:

For convective heat flow:

$$\rho_w C_w b \frac{\partial T}{\partial t} + C_w \frac{q}{h} \frac{\partial T}{\partial x} = 2k \frac{\partial T}{\partial y} \tag{6}$$

where ρ_w is the density of the water in the fracture, C_w is the heat capacity of the water in the fracture, b is the width of the fracture, T is the temperature of the fracture, t the time, q the injected flow rate, h the height of the fracture, x the distance from injection well along the fracture, k the thermal conductivity of the reservoir and y the direction perpendicular to the fracture plane (representation in Figure 8).

For conductive flow:

$$\frac{\partial^2 T}{\partial t^2} = \frac{\rho_r C_r}{k} \frac{\partial T}{\partial t} = \frac{1}{\alpha} \frac{\partial T}{\partial t} \tag{7}$$

where ρ_r is the density of the reservoir fluid, C_r is the heat capacity of the reservoir and α is the thermal diffusivity.

A solution for these equations is given by Carslaw and Jaeger (1959)

$$T_{out}(x,t) = T_{inj} + (T_0 - T_{inj})\, erf\left[\frac{kxh}{C_w q \sqrt{\alpha \left(t - \frac{x}{\beta}\right)}}\right] \tag{8}$$

and is valid at times $t > x/\beta$ where β is defined by $q/(\rho_w\, h\, b)$, where q is as before the injection flowrate in the fracture zone. T_{out} is the fracture outlet temperature and T_0 is the initial temperature of the reservoir.

The production temperature of a well of flowrate $Q > q$ finally is given by :

$$T(t) = T_0 - \frac{q}{Q}[T_0 - T_{out}] \tag{9}$$

In order to get an estimate of the additional mass of high pressure steam, the outlet temperature results from TRCOOL are used and the enthalpy values for water and steam corresponding to 6 bar-a separator pressure.

The equation of mass conservation for the fracture zone flow to the separator is

$$h_t = h_w(trcool) = x h_s + (1-x) h_w \tag{10}$$

$$x = \frac{C_w T(trcool) - 675}{2756 - 675} \tag{11}$$

Finally, the mass of steam is given as q*x (steam fraction).

7.2 Predicting cooling and thermal efficiency

As mentioned earlier, most of the Ahuachapán tracer tests yielded low recovery of the injected tracer. This low recovery makes the fracture heat flow model questionable as other flow channel geometries may exist. It was therefore decided to limit the TRCOOL simulations to Test #1 when fluid was injected in well AH-5 and 28% of the tracer was recovered in well AH-1, and Test #4 when fluid was injected in well AH-29 and 4.6% of the tracer recovered in AH-20. The TRINV values for the AH 5 → AH-1 dipole and AH-29 → AH-20 dipole (Table 4) were used for several case studies for different injection flow rates and temperatures, fracture thickness, height and porosity.

TABLE 5: TRCOOL outlet temperature results

Test # 1 AH-5 -> AH-1				
All Channels				
INPUT: Tinj.=160°C	Tfor.=220°		por=50%	A*por=79m^2
File: sc		b=1 m	H=158 m	
Q (kg/s)	Years			
	1	2	5	10
1	220	220	220,0	219,5
2	220	219,9	216,1	207,5
5	215,6	205,5	191,3	182,7
10	195,5	185,6	176,4	171,6
Test # 1 AH-5 -> AH-1				
All Channels				
INPUT: Tinj.=160°C	Tfor.=220°		por=50%	A*por=79m^2
File:sca		b=2 m	H=79 m	
Q (kg/s)	Years			
	1	2	5	10
1	220	220	217,3	208,5
2	219,9	214,2	198,7	188,3
5	197,8	186,5	176,6	171,7
10	179,2	173,3	168,3	165,8

Tables 5 and 6 show some of the results for these sensitivity analysis using different values of h, b and ϕ. The results are plotted in Figures 17 to 22. The different values of the fracture geometry are classified here into 6 cases. The main results are as follows (cases A to F).

Case A: The well dipole AH-5 →AH-1 and fracture width of 1 m (Test #1)

$Tinj$ = 160°C; $Tfor$ = 220°C; q = variable; ϕ = 50%; $A\ \phi$ = 79 m^2; b = 1 m; h = 158 m.

The cooling predictions shown in Figure 17 have been chosen as the most reasonable representation of the fracture zone connecting the two wells (using b=1 m and ϕ=50%). The cooling calculated by 2 kg/s of injection flow rate in a fracture, in 10 years of continuous injection is around 12°C, declining from the initial 220°C reservoir temperature to around 208°C. For 1 kg/s the temperature remains constant.

TABLE 6: TRCOOL additional steam and thermal recovery results

Test # 1	AH-5 -> AH-1							
All Channels								
INPUT:	Tinj.=160°C,	Tfor=220 °C,	por=50%	A*poro=79 m^2,		b=1 m,		H=158 m
File: scas								
Years	Additional high pressure steam (kg/s)				Additional power (MW)			
	1 kg/s	2 kg/s	5 kg/s	10 kg/s	1 kg/s	2 kg/s	5 kg/s	10 kg/s
1	0,12	0,24	0,55	0,70	0,30	0,60	1,38	1,75
2	0,12	0,24	0,45	0,50	0,30	0,60	1,12	1,25
5	0,12	0,22	0,31	0,31	0,30	0,56	0,77	0,79
10	0,12	0,19	0,22	0,22	0,30	0,47	0,55	0,55
Test # 1	AH-5 -> AH-1							
All Channels								
INPUT:	Tinj.=160°C,	Tfor=220 °C,	por=50%,	A*poro=79 m^2		b=2 m,		H=79 m
File: scasa								
Inj. flow rate (kg/s)	Additional high pressure steam (kg/s)				Additional power (MW)			
	1 kg/s	2 kg/s	5 kg/s	10 kg/s	1 kg/s	2 kg/s	5 kg/s	10 kg/s
1	0,12	0,24	0,37	0,37	0,30	0,60	0,93	0,93
2	0,12	0,22	0,26	0,25	0,30	0,54	0,65	0,63
5	0,11	0,15	0,16	0,15	0,28	0,38	0,40	0,38
10	0,10	0,11	0,11	0,10	0,24	0,28	0,28	0,26

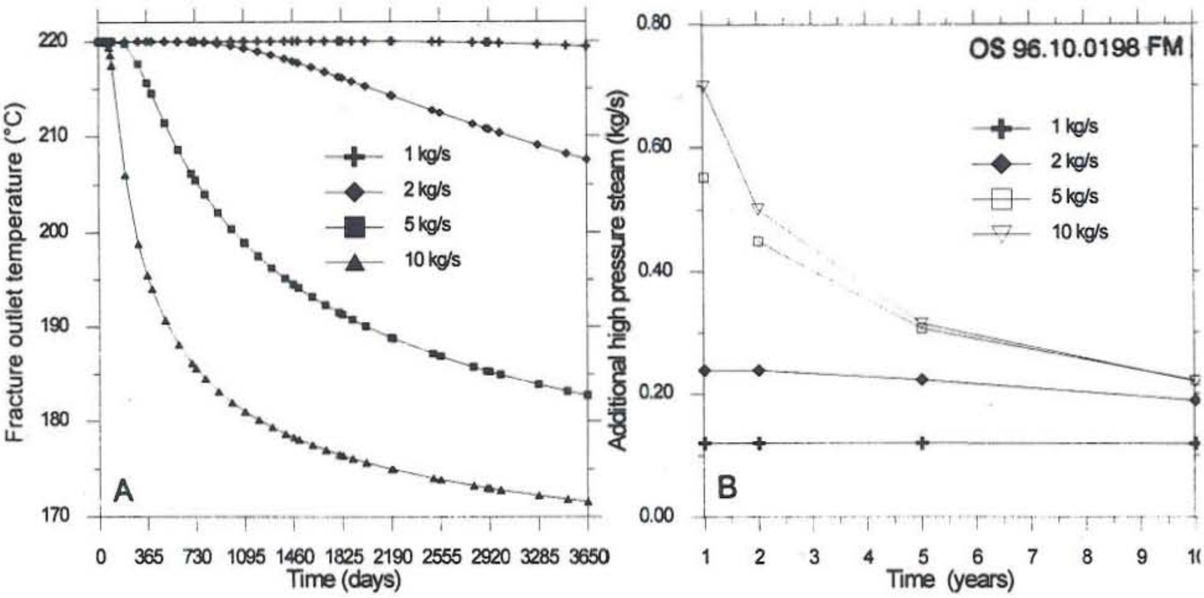

FIGURE 17: Case A, a) Predicted outlet temperature; b) Additional high-pressure steam

It should be stressed that 1 to 3 kg/s, as a fluid flow in fracture, represents around 10 kg/s of total injected fluid in the injector well as only 30% of the injected tracer was recovered in well AH-1. The additional high pressure steam result is close to 0.24 kg/s giving about 0.1 MWe gain in electrical power (a conversion factor of 2.5 kg/s/ MWe is assumed).

Case B: The well dipole AH-5→AH-1 and fracture width of 2 m (Test #1)

$Tinj$ = 160°C; $Tfor$ = 220°C; q = variable; ϕ = 50%; $A\ \phi$ = 79 m^2; b = 2 m; h = 158 m.

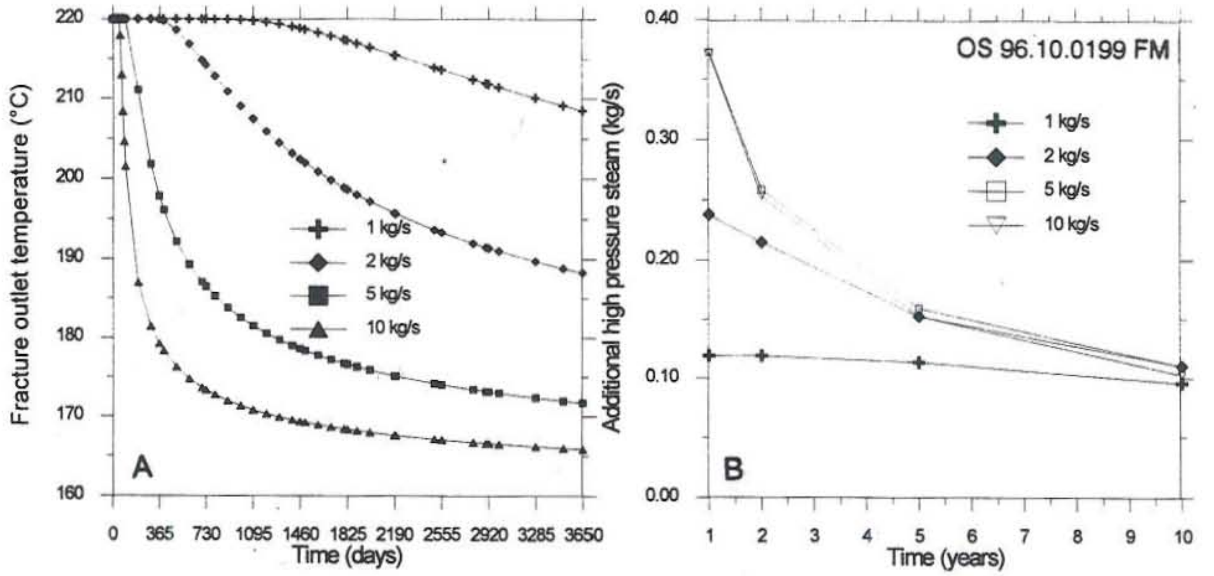

FIGURE 18: Case B, a) Predicted outlet temperatures; b) Additional high pressure steam

In this case a wider fracture zone is considered. The results show a slightly increased cooling as compared to case A (Figure 18). A continuous injection for 2 years of 2 kg/s reduces the fracture outlet temperature by 6°C (from 220 to 214°C).

Case C: The well dipole AH-5→AH-1 and 100% porosity of fracture zone(Test #1)

Tinj = 160°C; *Tfor* = 220°C; q = variable; ϕ = 100%; $A\ \phi$ = 79 m^2; b = 1 m; h = 79 m.

Here an increase of the fracture zone porosity to 100% is studied (Figure 19). The results are identical to case B, as should be expected. The reason is that the fracture height, h, will be the same for both models, given that the product $hb\phi$ is constant (79 m ^{2}).

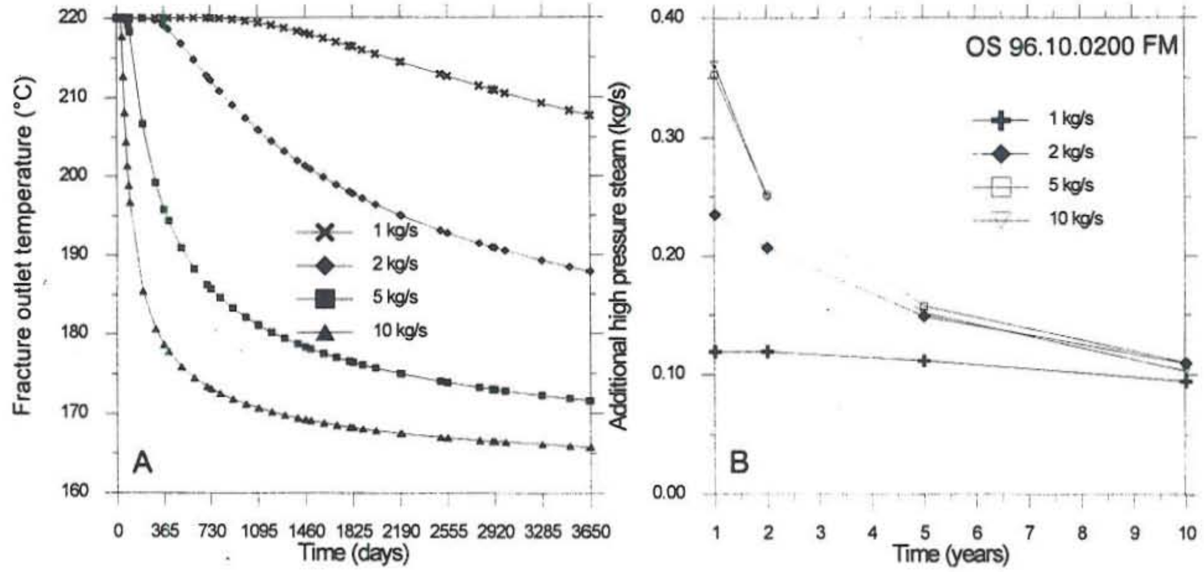

FIGURE 19: Case C, a) Predicted outlet temperatures; b) Additional high-pressure steam

Case D: The well dipole AH-5→AH-1 and large fracture width and porosity (Test #1)

Tinj = 160°C; *Tfor* = 220°C; q = variable; ϕ = 100%; $A\ \phi$ = 79 m^2; b = 2 m; h = 40 m.

In this case a fracture porosity of 100% and fracture width of 2 m is assumed (Figure 20). The cooling is around 22° by injecting constantly 2 kg/s water at 160°C for 2 years The additional steam gain in this case is 0.13 kg/s providing a 0.05 MWe gain in electrical power.

This case can be taken as the most pessimistic one studied. It should also be stressed that the calculation of additional high pressure steam is approximate since we only know the product of the fracture cross-sectional area.

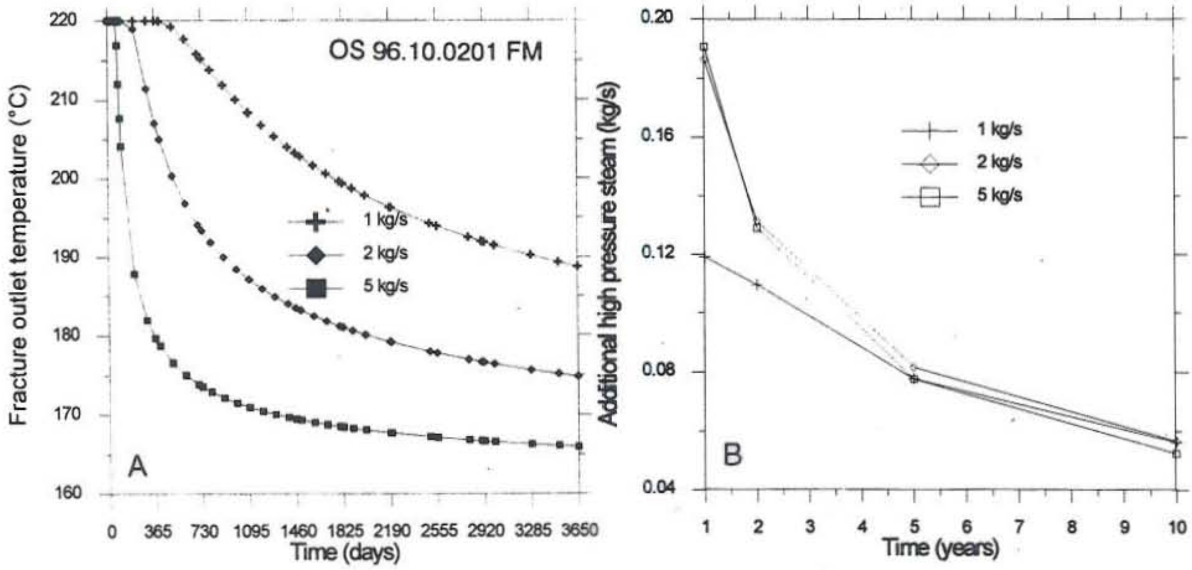

FIGURE 20: Case D, a) Predicted outlet temperatures; b) Additional high-pressure steam

Case E: The well dipole AH-5→AH-1 and the reduced temperature of the injected fluid (Test #1)

Tinj = 100°C; *Tfor* = 220°C; q = variable; ϕ = 50%; $A\ \phi$ = 79 m^2; b = 2 m; h = 79 m.

In this case, a 100°C water temperature is used for the injection (Figure 21) This gives similar cooling and steam gain as in case A for 1-2 kg/s injection rates. The explanation could be that the time is too short to have more cooling and that the water at 100°C is more efficiently extracting the heat from the rock. With higher injection rates, however, reservoir cooling becomes substantial. Finally the fracture outflow temperature falls below the temperature of the high-pressure steam separator. This leads to negative values for the additional high-pressure steam (Figure 21b). The meaning of these negative values is that the injected fluid takes heat from other feed zones in the well, which consequently reduces the total electrical output of the well compared to the no injection situation.

Case F: The well dipole AH-29→AH-20 and variable injection and reservoir temperatures (Test #4)

Tinj = 100-160°C; *Tfor* = 180-225°C; q = 2 kg/s; ϕ = 50%; $A\ \phi$ = 50 m^2; b = 2 m; h = 50 m.

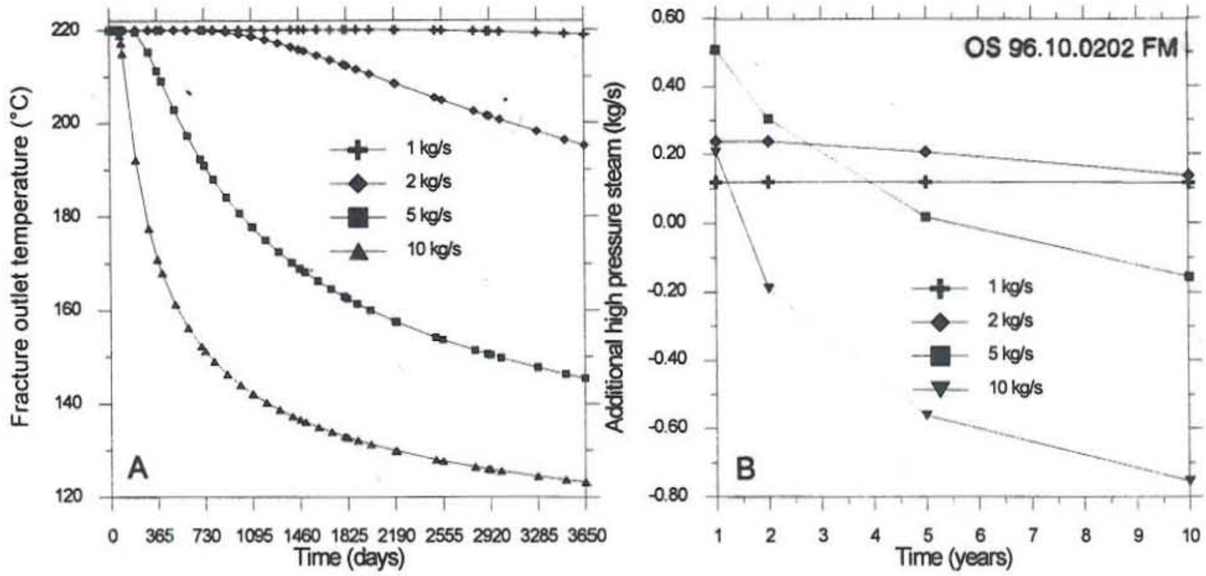

FIGURE 21: Case E, a) Predicted outlet temperatures; b) Additional high-pressure steam

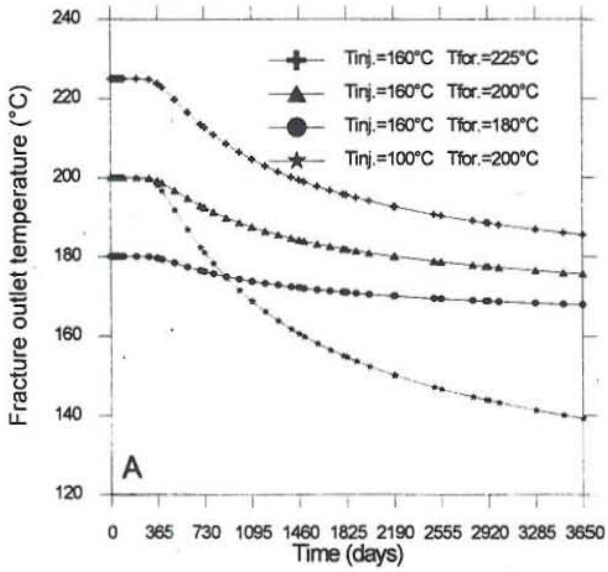

In this case, different formation and injection temperatures are studied. The fracture porosity (50%) and the injection flow rate (2 kg/s) are, however, kept constant. The flow rate is 5% of the 50 kg/s injection in AH-29, as is the cumulative tracer recovery. As should be expected, the higher the reservoir temperature the higher the thermal recovery. It is also worth mentioning that injection of 100°C water will only provide additional steam for 4 years. The results are shown in Figure 22.

The comparison of the results of the simulations using different values for several parameters shows a logical consistence regarding the cooling

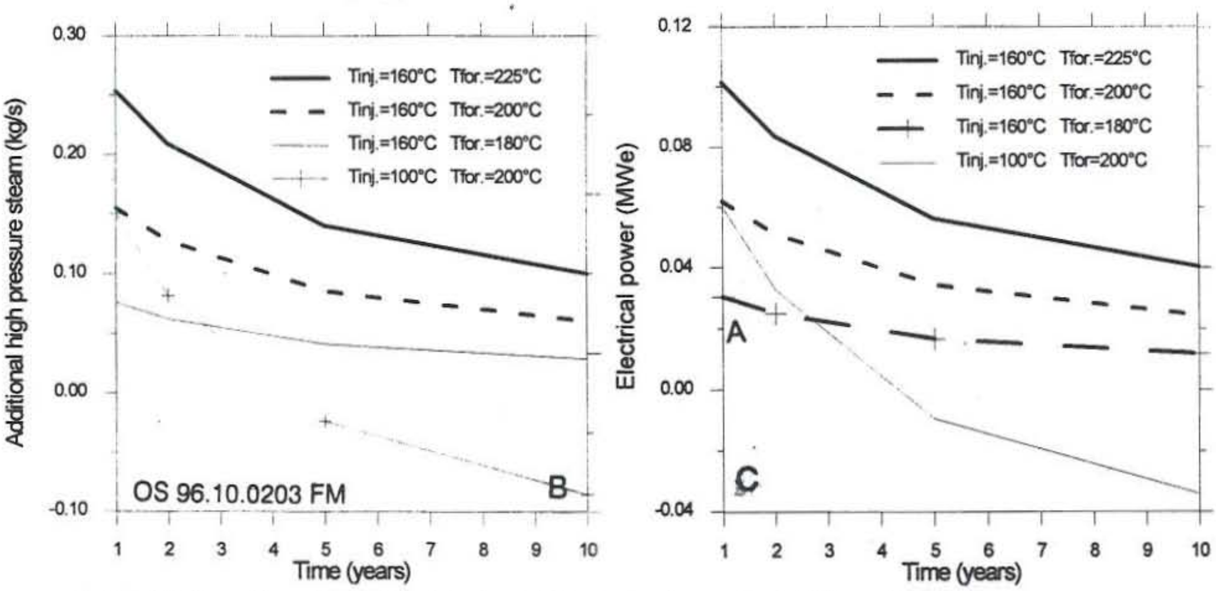

FIGURE 22: Case F, a) Predicted outlet temperatures; b) Additional high-pressure steam; c) Gain in electrical power

and the characteristics of the flow fracture channel. Low values of the cross-sectional area of the fracture together with high fracture porosity and large fracture width, result in low thermal recovery from the fracture. In the case of narrow fracture, the height of the fracture is increased producing more fluid dispersion and hence less cooling in the fracture, as the contact area between the fluid and the fracture becomes large. In cases of extremely low values of fracture cross-sectional areas (from TRINV results) the TRCOOL model produces an unrealistic cooling because the $A\phi$ parameter does not represent a fracture zone cross-sectional area but rather a matrix flow character. This makes the fracture model approach for cooling predictions unrealistic.

It should be stressed that the fracture model presented here is a pessimistic approach. We must also take into account the short distance between wells and the rapid tracer breakthrough time which produces the low thermal efficiency. Finally, it should be remembered that the low tracer recoveries indicate long travel time and efficient thermal recovery for a large fraction of the injected water.

8. TRACER RESULTS AND THE CONCEPTUAL RESERVOIR MODEL

Figure 23 shows mean tracer velocities for all the Ahuachapán experiments analysed in this work. The results of the tracer experiments in the S-SE and N-NE sector of the well field are in agreement with the present natural state model (Figure 2) showing that the fluid moves from the southern part through the centre of the field with velocities more than 10 times higher than in the northern part. This could mean that a significant recharge of mass takes place in the south and, hence, reaches the reservoir more rapidly than the colder water recharge from the N-NE. That is also in agreement with chemical modelling studies (Montalvo, 1994, 1996a).

The results for the northeastern part, mainly the I^{125} (long term) experiment show that this zone can be beneficial as an injection site. Only a small part of the tracer (8% for the Test # 4) comes to the reservoir without significant effects in well outputs (Maltez, 1993). Information regarding these effects is not available for the Test # 1.

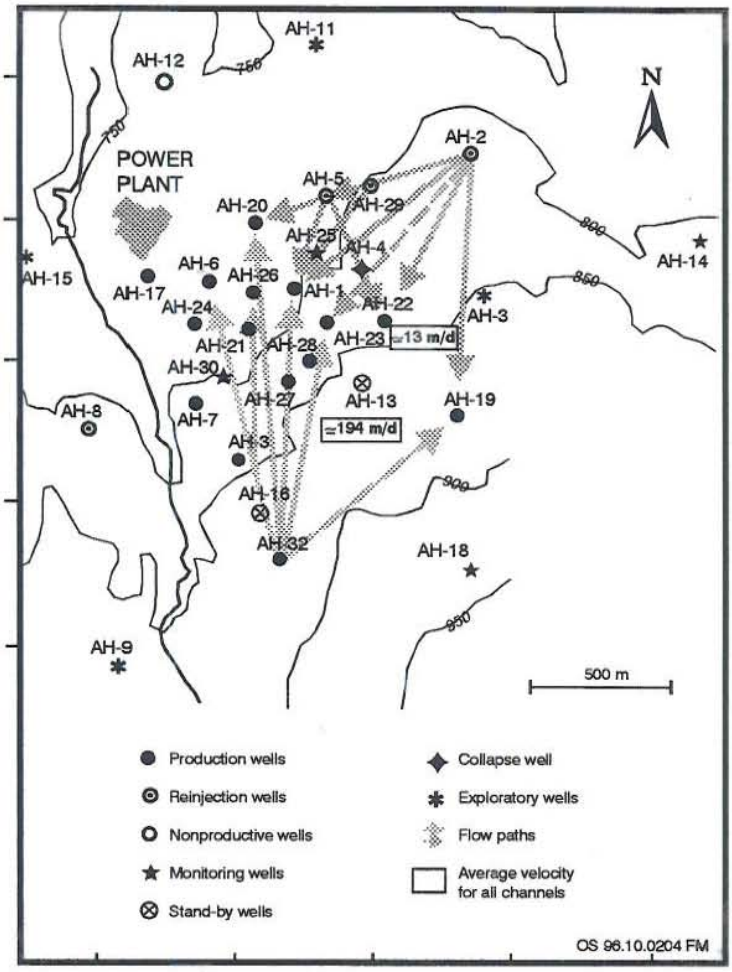

FIGURE 23: Mean tracer velocities for the Ahuachapán well field

9. DISCUSSION AND RECOMMENDATIONS

Erratic tracer results for many of the tracer tests carried out at Ahuachapán are possibly due to changes in the velocity flow field of the reservoir, as operation conditions of the well were often changed during the test (McCabe et al., 1990). An absolute requirement for the success of subsequent tests is therefore to maintain steady production-injection rates some weeks before and through the experiment. The water flow rate and enthalpy data (monthly average) show that there have never occurred dramatic changes in the production parameters. An example of that is well AH-1 in the period of the tracer experiments. It is suggested that a detailed analysis of the well field operation should be carried out in order to possibly reduce the scattering in the tracer data observed in almost all the tests. Also a complementary analysis regarding the chemistry changes in the period of the experiments could be useful for clarifying this situation.

It should be noted that the data scattering may also be a product of the complex structure (fracture and matrix porosity) in the reservoir The low tracer recovery could also be due to high dilution of the tracer (dispersion) or mixing in some relative large volume (not fracture) in the reservoir.

Some suggestions about the possibility of systematic error in the analysis, due to contamination or counter instability including negative background values, have been also mentioned by McCabe et al. (1990). McCabe et al. also suggested that in some cases peak concentration may not have been reached when the test was stopped. This means that the average residence time of the tracer in the reservoir is greater than the duration of the test and the calculated percentage tracer and hence return of injected water should be at least two or three times higher The author agrees with these observations because the total recovery is so low, that a substantial fraction of the injected fluid may have reached the production zone after the tracer monitoring So extending the monitoring is suggested, at least for one month in order to get the tail of the recovery curves that is so badly missing for most of the tracer tests.

10. CONCLUSIONS

The several tracer tests that have been carried out in the Ahuachapán geothermal field show that the cumulative tracer recovery is generally in the range of 0-28% (almost all the monitoring wells exhibit tracer recoveries of less than 1%). Modelling studies for selected well dipoles show coefficients of determination higher than 90% which means good matching between observed and calculated data by the TRINV program The results suggest the presence of generally two main fracture channels connecting injection and production wells. These may represent a fracture-dominated zone and matrix-dominated flow channels.

Calculated tracer velocities support lateral fluid recharge to the well field in accordance with the conceptual model of the system (flow from S to N) and colder water inflow into the reservoir (from the N-NE). The latter seems to be less significative according chemical modelling studies.

Due to lack of field-laboratory information and the scattered tracer recovery data, it is difficult to pinpoint the fracture model properties. The available information does not suggest that the scattered results could be explained by significant changes in operating conditions of the monitoring wells for the period of the tracer monitoring. Some of the scattering of results could be associated with the sampling procedure and analysis errors due to the difficulties regarding the manipulating of radioactive samples and unknown sources of interference, contamination or performance of the equipment.

TRCOOL predictions suggest that a small scale injection in the well field is beneficial for the operation of the field. Large scale injection will however lead to rapid cooling of the reservoir (as was observed when the large scale injection was applied in 1975-1982) Lower injection rates (1-3 kg/s) of 160°C water give, however, a low but stable recovery of electrical power (0.05-0.1 MW).

Even though the present analysis are a pessimistic approach regarding the fracture nature of the model, relatively little cooling and some additional steam recovery should be expected if the water at separator pressure (even at 100°C) is injected at low flow rates and for moderate period of time (less than 2 years). The low calculated values of thermal recovery are due to the short distance between the wells (no more than 500 m in this case) and a small contact area between the fluid and the rocks. Most benefits using the injection should be obtained if the injection takes place further away. That may allow large scale injection for long time.

For the cases of negligible tracer recovery and low cross-sectional area of the fracture, the thermal model does not apply. This explains an unrealistic reservoir cooling using TRCOOL.

11. FUTURE TESTING PROCEDURE

The following suggestions apply for carrying out new tracer test experiments in the Ahuachapán geothermal area:

- Steady state operation of the field (production and injection) before and after the tracer injection and through the monitoring period;
- The security about the full performance of the tracer experiments should be settled;
- Careful selection of sampling points (wells and springs);
- Start collection of water samples before the tracer injection and extend the monitoring in the wells showing tracer recovery until tracer concentration are down to the background values;
- Careful determination of background radiation;
- Register time of each sampling and of analysis;
- Register information on water flow rates and enthalpies in monitoring wells during sampling;
- Avoid contamination and analytical errors;
- Improve statistical analysis for the laboratory processing;
- Make sure that all relevant information regarding the tracer testing is stored;
- Make a correlation with chemistry and production data;
- Select the best recovery curves for studying geometrical and hydrological properties of the formation (channels between injection-production well dipoles) ;
- Predict thermal efficiency of the injection and estimate heat mining by fracture model calculations.

ACKNOWLEDGEMENTS

I would like to thank to the Comisión Ejecutiva Hidroeléctrica del Río Lempa (CEL) - Gerencia de Recursos Geotérmicos for giving me the permission to participate in this training Special thanks to International Atomic Energy Agency (IAEA) in Vienna, for providing me with this Fellowship, extended to Ms. Jane Gerardo at IAEA for her suggestions about the tracers. I would like thank my advisors Mr. Benedikt Steingrímsson and Mr. Grímur Björnsson for sharing their experience and excellent guidance during my training. Extended thanks to Mr. Árni Ragnarsson and Mr. Lúdvik S. Georgsson for providing me with hardware-software facilities for the preparation of my lecture about this project.

Special thanks to Dr. Ingvar Fridleifsson for his acceptance to my Fellowship, that did my stay possible at the UNU - Geothermal Training Programme.

REFERENCES

Arason, P., and Bjornsson G., 1994: *ICEBOX.* 2nd edition, Orkustofnun, Reykjavík, 38 pp.

Axelsson, G., Björnsson, G., Flóvenz Ó.G., Kristmannsdóttir, H., and Sverrisdóttir, G., 1995: Injection experiment in low-temperature geothermal areas in Iceland. *Proceedings of the World Geothermal Congress, Florence, Italy, 3,*1991-1996.

Bustillo, M., 1996: *Síntesis de las pruebas de radiotrazado ejecutadas en los campos geotérmicos de Ahuachapán y Berlín.* CEL, El Salvador, internal report (in Spanish).

Carslaw, H.S., and Jaeger, J.C., 1959: *Conduction of heat in solids.* 2nd Edition, Oxford University Press, Ely House, London, 510 pp.

ELC, 1993: *Factibilidad del programa integral de estabilización para el campo geotérmico de Ahuachapán - Informe de evaluación del recurso.* Electroconsult, internal report (in Spanish) submitted to CEL, El Salvador.

Maltez, J., 1993: *Area de Isótopos. Síntesis de las pruebas de radiotrazdo en el cuadrante N-E del campo geotérmico de Ahuachapán 1987/1992.* CEL, El Salvador, internal report (in Spanish).

McCabe, W.J, 1987: *Interpretation and evaluation of data resulting from the injection of Iodine-131 in the Ahuachapán geothermal field.* IAEA, Special service agreement between IAEA and Institute of Nuclear Sciences, New Zealand.

McCabe, W.J., 1991: *AH-2 reinjection tracer test, Ahuachapán, El Salvador.* Nuclear Sciences Group, DSIR Physical Sciences, Lower Hutt, New Zealand.

McCabe, W.J., Mayen, E., and Hernández, P., 1990: *Avance de las pruebas de Radiotrazdo en el campo geotérmico de Ahuachapán.* CEL, El Salvador, internal report (in Spanish).

Montalvo L., F.E., 1994: Geochemical evolution of the Ahuachapán geothermal field, El Salvador C.A. Report 9 in: *Geothermal Training in Iceland 1994,* UNU G.T.P., Iceland, 211-236.

Montalvo L., F.E., 1996a. *20 anos de explotación del Campo Geotérmico de Ahuachapán.* CEL, El Salvador, internal report (in Spanish).

Montalvo L., F.E., 1996b: *Appendix to the report:Geochemical evolution of the Ahuachapán geothermal field, El Salvador C.A.* UNU G.T.P., Iceland, report 9 appendix, 35 pp.

Quijano C., J.E., 1994: A revised conceptual model and analysis of production data for the Ahuachapán-Chipilapa geothermal field in El Salvador. Report 10 in: *Geothermal Training in Iceland 1994,* UNU G.T.P., Iceland, 237-266.

Steingrímsson, B., Aunzo, Z., Bödvarsson, G.S., Truesdell, A.H., Cuéllar, G., Escobar, C., and Quintanilla, A., 1991: Changes in thermodynamic conditions of the Ahuachapán reservoir due to production and injection. *Geothermics, 20,* 23-38.